



## Application of heterogeneous Fenton processes using Fe(III)/MnO<sub>2</sub> and Fe(III)/SnO<sub>2</sub> catalysts in the treatment of sunflower oil industrial wastewater

Sefika Kaya, Yeliz Asci\*

Department of Chemical Engineering, Eskisehir Osmangazi University, Eskisehir, Turkey,  
emails: yelizbal26@gmail.com/yelizbal@ogu.edu.tr (Y. Asci), sefikakaya@ogu.edu.tr (S. Kaya)

Received 2 April 2019; Accepted 14 August 2019

---

### ABSTRACT

The treatment of industrial wastewater is one of the most important problems to be considered today. In recent years, advanced oxidation processes based on the production of hydroxyl radicals with high oxidation potential are preferred in the treatment of wastewaters. In this study, color and chemical oxygen demand (COD) removal efficiencies of sunflower oil industrial wastewater have been investigated by applying a heterogeneous Fenton process. Fe(III)/MnO<sub>2</sub> and Fe(III)/SnO<sub>2</sub> catalysts have been prepared by the co-precipitation method and characterized by scanning electron microscopy and Brunauer–Emmet–Teller techniques. The effects of the amount of the catalyst, pH, hydrogen peroxide concentration, temperature, reaction time and mixing speed on the process have been studied and the optimum conditions have been determined. In the heterogeneous Fenton process, 98% color and 89% COD removal efficiency for Fe(III)/MnO<sub>2</sub> catalyst and 92% color and 67% COD removal efficiency for Fe(III)/SnO<sub>2</sub> catalyst have been obtained. This result indicates that Fe(III)/MnO<sub>2</sub> catalyst is more effective in the treatment of sunflower oil industrial wastewater. The stability and reuse of the catalysts have also been tested. These catalysts successfully overcome the two problems encountered during the heterogeneous Fenton process. They are reusable and there has been no significant reduction in the efficiency of the catalysts even after four consecutive runs.

*Keywords:* Heterogeneous Fenton; Oxidation; Sunflower oil; Industrial wastewater; Catalyst

---

### 1. Introduction

After the industrial revolution, rapid global economic growth created such problems as a clean water crisis and environmental pollution [1]. The demand for clean water has increased day by day due to the rapid increase in the population and it has become a serious problem that must be solved first [2]. The contamination of water on earth is caused by an uncontrolled discharge of untreated and/or partially treated industrial wastes [3].

Until now, traditional wastewater treatment techniques such as biological treatment (biodegradation) and physical and Physico-chemical treatment (flocculation, chlorination,

and ozonation) have been widely used in wastewater treatment. These methods have been reported as inadequate to remove organic pollutants in wastewater [2]. The presence of non-biodegradable organic compounds in water poses a serious threat to human health. It has known that more amounts of these organics are toxic, endocrine-disrupting, mutagenic and potentially carcinogenic to humans, animals and aquatic life in general. Many organic pollutants are also considered as toxic and harmful even at lower concentrations [3].

Insufficient to bring wastewater pollution to discharge standards, traditional treatment methods and increasing

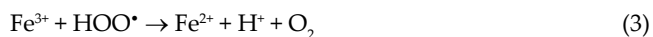
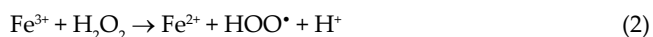
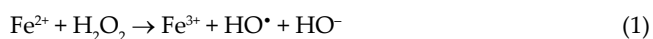
---

\* Corresponding author.

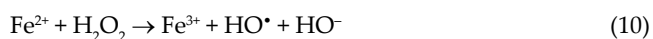
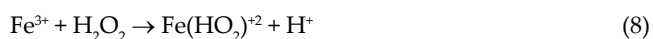
treatment costs have led the industry to seek more effective water treatment approaches. Many studies show that advanced treatment technologies are needed for water and wastewater treatment and recovery [4–11].

Advanced oxidation processes (AOPs), having fewer operating problems and higher treatment efficiency than other advanced treatment methods, have come to the forefront in recent years as methods for industrial wastewater treatment [8]. The AOPs offer alternative methods that provide high yields to reduce or even mineralize organic pollutants resistant to biological degradation [12].

The AOPs use highly reactive hydroxyl radical as an oxidizing agent and thus provide effective oxidation processes for the complete removal of organic contaminants from aqueous solutions. Hydrogen peroxide has many outstanding properties such as being non-selective, rapid reaction kinetics, cheap and safe and having a high potential of oxidation. The oxidation of organic compounds by hydroxyl radicals is rapid and results in the oxidation of contaminants to primarily carbon dioxide and water. Hydrogen peroxide and iron ion reaction is a classic Fenton process. The Fenton process uses ferrous ion as the catalyst to generate hydroxyl radicals from hydrogen peroxide [13,14]. The Fenton reactions are as follows [15]:



The disadvantages of classic Fenton processes such as sludge formation and iron ion recovery due to high levels of iron discharge led the studies to heterogeneous Fenton processes [16]. The heterogeneous Fenton reaction takes place at the surface of the catalyst and the rate of production of the hydroxyl radicals varies depending on the iron oxide surface area, pore size and hydrogen peroxide concentration [17].



Catalysts can both retain the ability to form hydroxyl radicals from hydrogen peroxide, and the formation of iron hydroxide precipitates is prevented. In addition to the limited dissolution of iron ions, the catalysts can be easily recovered after the reaction and remain active during subsequent processes [18].

The commonly used catalysts in studies on AOPs are iron minerals such as hematite [19,20], pyrite [21–25], goethite [26–28], and zeolite [29,30] which are abundant on earth and are magnetically separated from the reaction medium [1]. In recent years, semiconductor metal oxides are preferred as catalysts in AOPs. Metal oxide semiconductors have positive valence band potentials compared to other semiconductors. Therefore, metal oxide semiconductors form voids with high oxidation potentials and thus oxidizing almost all chemical substances [31,32]. Also, semiconductor metal oxides have such advantages as chemical stability, ease of production in high amounts, high porosity, reusability, high affinity for many molecules and water, non-toxic and non-biologically active [33,34]. Semiconductor metal oxides such as  $\text{TiO}_2$  (3.2 eV),  $\text{ZnO}$  (3.4 eV),  $\text{SnO}_2$  (3.6 eV), and  $\text{WO}_3$  (2.8 eV) have frequently been investigated as catalysts in AOPs in wastewater treatment [34–46].

$\text{MnO}_2$  is stable at low pH and can react with aqueous  $\text{H}_2\text{O}_2$  solutions. However, it is a strong oxidant with a high oxidation potential of 1.23 eV. Therefore, the reaction between  $\text{H}_2\text{O}_2$  and heterogeneous manganese oxide has been frequently studied in an application containing AOPs [4].  $\text{MnO}_2$  has been used for the removal of many organic pollutants such as 4-chlorophenol [47], Methylene Blue [48,49], Rhodamine B, Congo Red, Ethylene Blue [50], tetrachloro-methane [51], phenol [52], carbon tetrachloride [53], Reactive Blue 19 [54] and hexachloro-ethane [55].

In the production of sunflower oil, the wastewater from the refining section contains considerable amounts of chemicals such as oil, soap, sodium hydroxide, sodium carbonate, phosphoric acid, and sulfuric acid. The release of these wastewaters into the environment leads to major problems. Particularly in aqueous environments, water cuts in contact with air, reducing the amount of oxygen in the water and posing a great danger to living beings [56]. These components discolor water and give it a nasty smell and taste and also increase the value of the chemical oxygen demand (COD) of water. COD value is one of the most important parameters used to determine the degree of organic pollution of industrial wastewater. The COD value is always higher than the need for biological oxidation since it shows both biological and chemically oxidizable organic pollution in the wastewater [57,58]. The biological treatment of sunflower oil wastewater is quite difficult since the bacteria that are active in biological treatment are coated with oil and grease and their activities are prevented [59]. Therefore, AOPs, which are much more effective than convection oxidizers in color removal and are capable of oxidizing all organic compounds without being selective, are preferred for the treatment of wastewater [60].

In the studies carried out for the treatment of sunflower oil wastewater, many treatment methods such as biological treatment [61–63], physicochemical treatment [64], electrocoagulation [65,66], membrane (ultrafiltration, microfiltration) [67–71] and sorption using bentonite [72], chitosan [73] and hydrophobic vermiculite [74] as adsorbents have been investigated.

In this study, the synthesis of  $\text{Fe(III)/MnO}_2$  and  $\text{Fe(III)/SnO}_2$  catalysts and the treatment of sunflower oil industrial wastewater with heterogeneous Fenton process were investigated using these catalysts. The effects of different operating

conditions such as catalyst amount, hydrogen peroxide concentration, initial pH, temperature, reaction time and mixing speed on color and COD removal efficiencies were investigated. The optimum conditions were determined according to the experimental results.

## 2. Materials and methods

### 2.1. Materials

The sunflower oil industry wastewater was obtained from an oil plant operating in Eskişehir. This wastewater was that which is sent to the treatment unit after neutralization in sunflower oil production. The characteristics of wastewater are given in Table 1. Hydrogen peroxide (30% w/w) and  $\text{Fe}(\text{NO}_3)_3 \cdot 9\text{H}_2\text{O}$  were supplied by Sigma-Aldrich (Germany) while  $\text{SnO}_2$  (99%) and  $\text{MnO}_2$  (99%) used in catalyst synthesis were purchased from Merck (Germany).

### 2.2. Methods

#### 2.2.1. Preparation of catalyst

$\text{Fe}(\text{III})/\text{MnO}_2$  and  $\text{Fe}(\text{III})/\text{SnO}_2$  catalysts containing 4, 8 and 12 wt.% Fe(III) were synthesized using the co-precipitation method for use in the heterogeneous Fenton process.  $\text{Fe}(\text{NO}_3)_3 \cdot 9\text{H}_2\text{O}$  and  $\text{MnO}_2/\text{SnO}_2$  were dissolved in 100 ml of distilled water and mixed in a heated magnetic stirrer. The pH was adjusted to 9 by dropwise addition of  $\text{NH}_4\text{OH}$  (26%) to the solution. After the addition of ammonium hydroxide was completed, the solution was stirred at 300 rpm for 2 h at 65°C constant temperature. The resulting precipitate was filtered and dried at 105°C for 24 h. The dried precipitate was left in an ash oven at 600°C for 2 h [75].

#### 2.2.2. Heterogeneous Fenton process

$\text{Fe}(\text{III})/\text{MnO}_2$  and  $\text{Fe}(\text{III})/\text{SnO}_2$  catalysts were used in experimental studies. First, the pH value of the wastewater sample was set to the desired value. The catalysts in the amounts specified were added to the sample and the  $\text{H}_2\text{O}_2$  solution was added and shaken in the shaking water bath at a constant temperature. At the end of the reaction period, the pH value of the sample was brought to 8. The sample was centrifuged to separate the catalyst and the solution. The solution was filtered and the necessary analyzes were carried out.

Table 1  
Parameters of wastewater

Parameters	Values
pH	9.5
COD (mg/L)	7,100
Color (Abs)	3.00
Suspended solids (mg/L)	1,127
Oil-grease (mg/L)	600
Conductivity ( $\mu\text{S}/\text{cm}$ )	1,631
Chloride (mg/L)	928

### 2.2.3. Color and COD analysis

In color analysis, the absorbance value and the maximum wavelength (359.2 nm) of the wastewater sample were determined by scanning in the spectrophotometer (Hach Lange DR 3900, Germany) in the wavelength range of 320–900 nm. The color analyzes of the samples were carried out at the determined wavelength and the removal efficiencies were calculated. In the analysis of COD, Hach Lange LCK 514 brand COD test kits were used. COD removal efficiencies were calculated by using spectrophotometer measurements.

## 3. Results and discussion

### 3.1. Catalyst results

$\text{Fe}(\text{III})/\text{MnO}_2$  and  $\text{Fe}(\text{III})/\text{SnO}_2$  catalysts containing 4, 8 and 12 wt.% Fe(III) ion were synthesized. The color and COD removal efficiencies of these catalysts on sunflower oil industrial wastewater were investigated experimentally. The results are given in Table 2.

Experimental studies were carried out with 8 wt.% iron ion-containing catalysts since the best color and COD removal efficiency were provided with these catalysts. Cihanoğlu et al. [14] used zeolite containing 8.5 wt.% iron ions within their study. Scanning electron microscopy (SEM) and energy distribution spectrometry (EDS) analyses were performed at the Central Research Laboratory of Eskişehir Osmangazi University to determine the surface morphology and elemental percentages of the  $\text{Fe}(\text{III})/\text{MnO}_2$  and  $\text{Fe}(\text{III})/\text{SnO}_2$  catalysts containing 8 wt.% iron ion. SEM images are shown in Figs. 1a and 2a and EDS results are given in Tables 3 and 4. The EDS spectra of the catalysts are indicated in Figs. 1b and 2b.

When the SEM images of the catalysts were examined, it was observed that the  $\text{Fe}(\text{III})/\text{MnO}_2$  catalyst have different-sized particles and intergranular voids.  $\text{Fe}(\text{III})/\text{SnO}_2$  catalyst has a spongy structure different from  $\text{Fe}(\text{III})/\text{MnO}_2$  catalyst.

Surface area analyzes of the synthesized  $\text{Fe}(\text{III})/\text{MnO}_2$  and  $\text{Fe}(\text{III})/\text{SnO}_2$  catalysts were carried out in Brunauer–Emmet–Teller method at Technology Research and Application Centre of Afyon Kocatepe University. The surface areas were determined using nitrogen adsorption isotherms with 7 points ( $p/p_0 = 0.01, 0.05, 0.10, 0.15, 0.20, 0.25, 0.30$ ) and the results are given in Table 5.

$\text{Fe}(\text{III})/\text{MnO}_2$  and  $\text{Fe}(\text{III})/\text{SnO}_2$  catalysts are in the range of mesoporous catalysts with pore sizes between 2 and 50 nm.

Table 2  
Removal results of catalysts containing iron ions in different percentages\*

Fe(III), wt.%	Color removal, %		COD removal, %	
	$\text{MnO}_2$	$\text{SnO}_2$	$\text{MnO}_2$	$\text{SnO}_2$
4	82.21	69.56	75.64	39.89
8	94.20	81.41	87.51	55.73
12	84.52	73.54	79.45	42.63

\*Experimental condition: pH = 2, catalyst amount 2 g/L,  $\text{H}_2\text{O}_2$  concentration 300 ppm, temperature 30°C, reaction time 120 min.

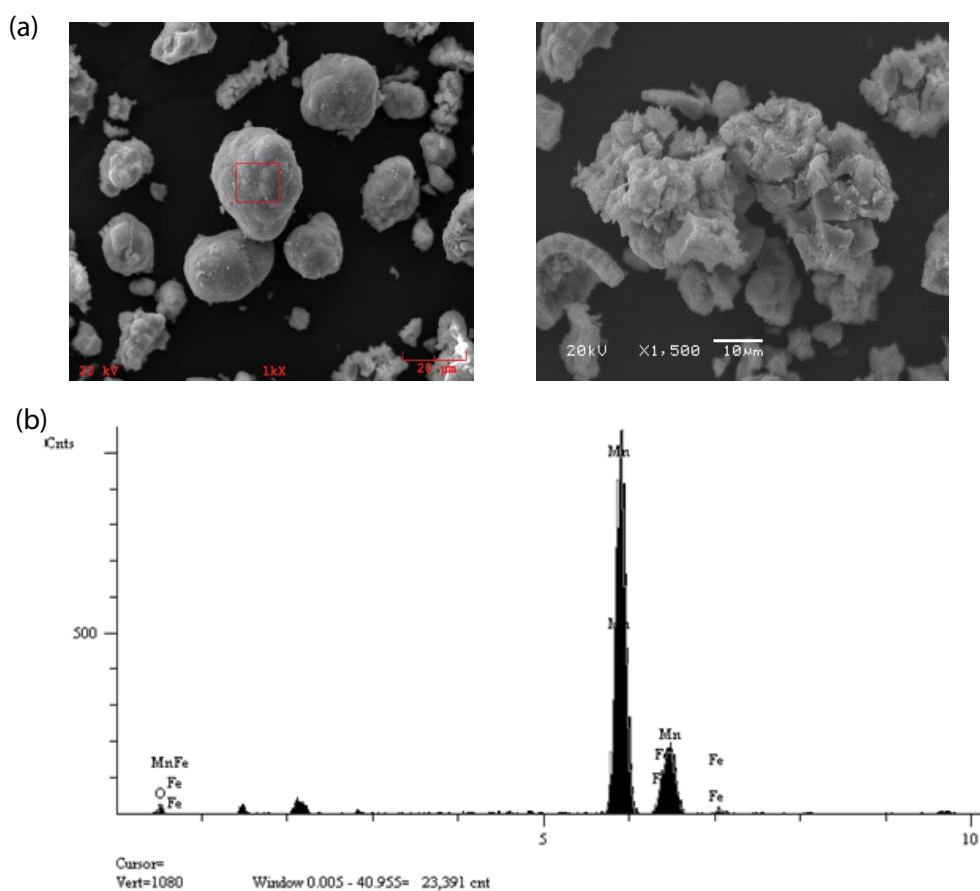


Fig. 1. (a) SEM image of Fe(III)/MnO<sub>2</sub> catalyst and (b) EDS spectra of Fe(III)/MnO<sub>2</sub> catalyst.

Table 3  
EDS elemental analysis of Fe(III)/MnO<sub>2</sub> catalyst

Component	Mole concentration	Concentration
Fe	8.44	8.89
O	5.00	1.51
Mn	86.56	89.60
Total	100.00	100.00

Table 4  
EDS elemental analysis of Fe(III)/SnO<sub>2</sub> catalyst

Component	Mole concentration	Concentration
Fe	11.65	8.45
O	33.46	6.95
Sn	54.89	84.60
Total	100.00	100.00

Due to the small pore sizes (<2 nm) of the microporous catalysts, their use as sorbents and catalytic materials for large molecular-weight organic compounds is limited [76]. Meso-porous catalysts have the greatest pore openings and are the least stressed of the mass transfer problems of compounds [77].

The size of the surface area depends largely on the size of the pores rather than the pore volume. As the pore size decreases, the surface area increases with the increasing number of walls. However, this does not result in the small pore volume of the small surface area [78].

The pore sizes of the catalysts we prepared were very close to each other. However, the surface area of Fe(III)/MnO<sub>2</sub> catalyst was determined to be approximately three times larger than the surface area of Fe(III)/SnO<sub>2</sub> catalyst. The reason of the surface area of Fe(III)/SnO<sub>2</sub> catalyst being low is that the Fe(III) cation reached to the inner surface of SnO<sub>2</sub> metal oxide and the nitrogen gas was only adsorbed on the outer surface.

### 3.2. Effect of the catalyst amount on the heterogeneous Fenton process

In the heterogeneous Fenton process experiments, the optimum catalyst amount was determined using Fe(III)/MnO<sub>2</sub> and Fe(III)/SnO<sub>2</sub> catalysts. When the effect of catalyst amount on color and COD removal was examined, the amount of catalyst was changed between 0.5 and 6.0 g/L. The other conditions such as pH, H<sub>2</sub>O<sub>2</sub> concentration, temperature and reaction time were constant.

One of the important parameters in the heterogeneous Fenton process is the amount of catalyst. The effects of Fe(III)/MnO<sub>2</sub> and Fe(III)/SnO<sub>2</sub> catalysts were investigated

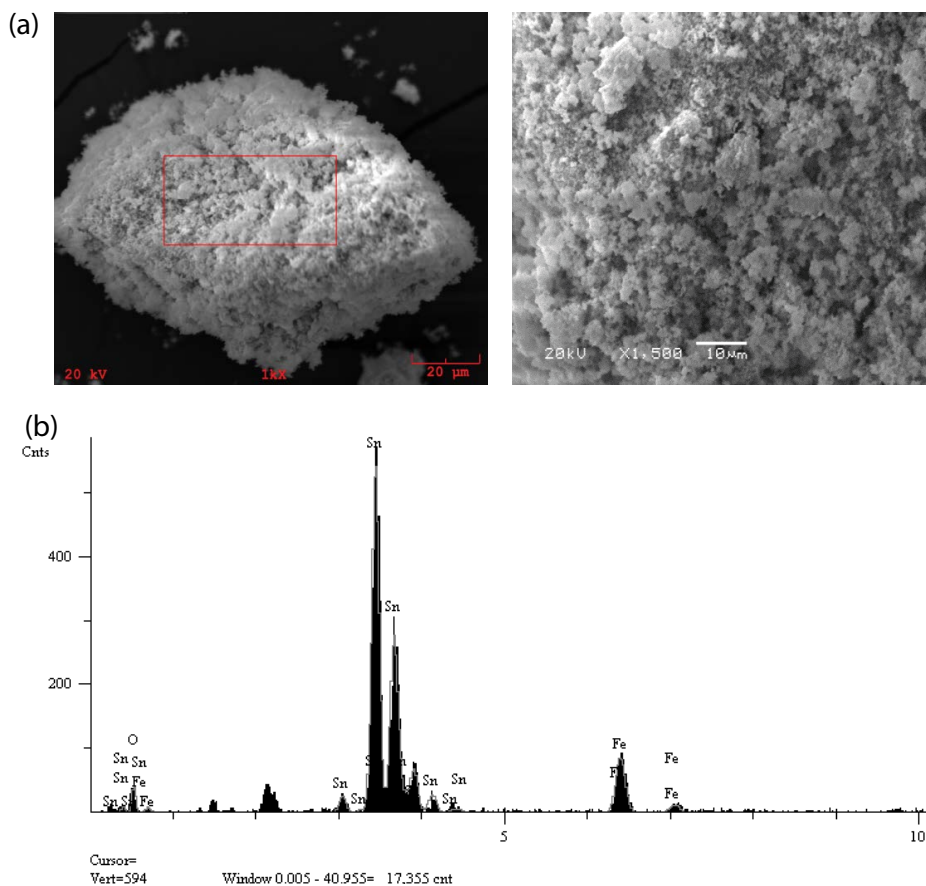


Fig. 2. (a) SEM image of Fe(III)/SnO<sub>2</sub> catalyst and (b) EDS spectra of Fe(III)/SnO<sub>2</sub> catalyst.

Table 5  
BET analysis results

	Fe(III)/MnO <sub>2</sub>	Fe(III)/SnO <sub>2</sub>
Surface area (m <sup>2</sup> /g)	30.91	9.30
Pore size (nm)	2.011	2.013

in different quantities in the sunflower oil industry wastewater removal studies. As the amount of catalyst increases, the active sites present on the catalyst surface increase and react with hydrogen peroxide to form more hydroxyl radicals [79]. After the optimum number of catalyst is added, a reversed tendency is observed, and as the number of catalyst increases, the iron ions form a sweeping effect on the hydroxyl radicals as given in the following equation [80].



As shown in Figs. 3 and 4, the color and COD removal efficiency in both catalysts increased with an increasing amount of catalyst and remained constant afterward. Experimental results show that Fe(III)/MnO<sub>2</sub> catalyst gives better results in color and COD removal. 1.5 g/L of Fe(III)/MnO<sub>2</sub> catalyst yielded 97.67% color and 88.66% COD while with 2.0 g/L of Fe(III)/SnO<sub>2</sub> catalyst 83.40% color and 66.55%

COD removal were obtained. In similar heterogeneous Fenton process studies, the optimum amount of catalyst was determined by Khataee et al. [81] as 3 g/L, Xu et al. [82] as 2 g/L, Zhao et al. [83] as 1 g/L and Muthukumari et al. [84] as 1 g/L.

### 3.3. Effect of the pH on the heterogeneous Fenton process

The pH affects the activity of the oxidant and the stability of the hydrogen peroxide [85]. Therefore, the effect of pH on color and COD removal efficiency was investigated. Experimental studies have been carried out with constant H<sub>2</sub>O<sub>2</sub>, temperature and reaction time in the quantities of catalysts. Studies were carried out at pH 1.5; 2; 3; 4; 5 and the results obtained are given in Figs. 5 and 6.

As shown in the figure, after the pH 3, the color and COD removal efficiencies were decreased for both catalysts. This is due to the formation of ferric hydroxide complexes at high pH values [86]. The resulting ferric hydroxide decomposes hydrogen peroxide into oxygen and water, resulting in a reduction of hydroxyl radicals and a lower oxidation potential of the hydroxyl radical [87]. Also, at high pH values, the reaction of the iron ion with hydrogen peroxide is slow and less amount of hydroxyl radical is produced [88]. Under acidic conditions, a high concentration of hydrogen ions can inhibit oxidation reaction by sweeping hydroxyl radicals in the medium [89,90]. Also, excess hydrogen ions can react

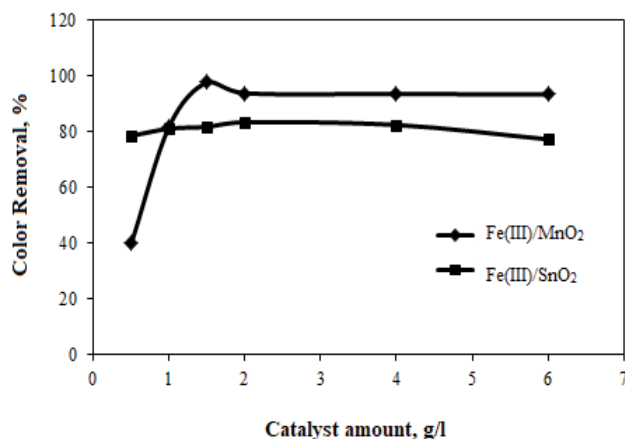


Fig. 3. Effect of the catalyst amount on color removal efficiency (pH = 2, H<sub>2</sub>O<sub>2</sub> = 200 ppm, temperature 30°C, reaction time 2 h).

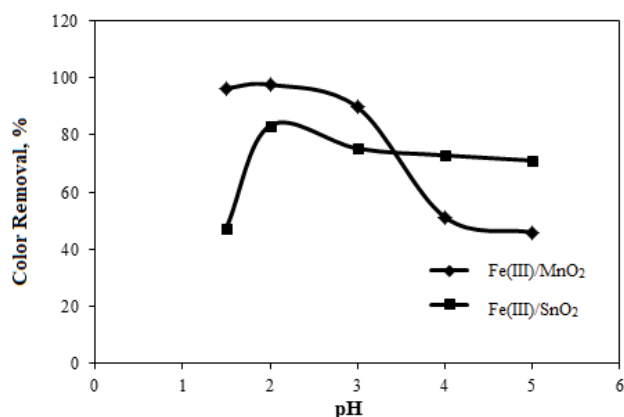


Fig. 5. Effect of the pH on color removal efficiency (Fe(III)/MnO<sub>2</sub> = 1.5 g/L – Fe(III)/SnO<sub>2</sub> = 2.0 g/L, H<sub>2</sub>O<sub>2</sub> = 200 ppm, temperature 30°C, reaction time 2 h).

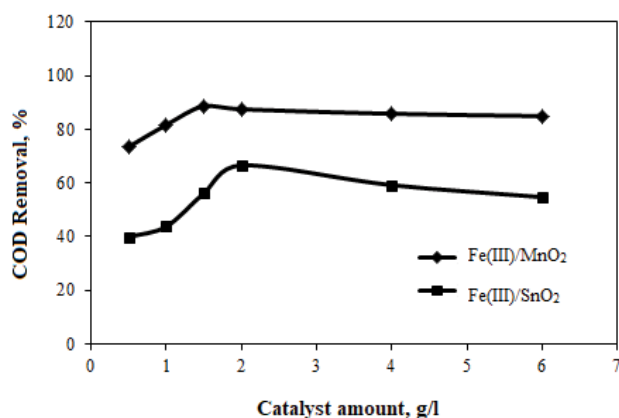


Fig. 4. Effect of the catalyst amount on COD removal efficiency (pH = 2, H<sub>2</sub>O<sub>2</sub> = 200 ppm, temperature 30°C, reaction time 2 h).

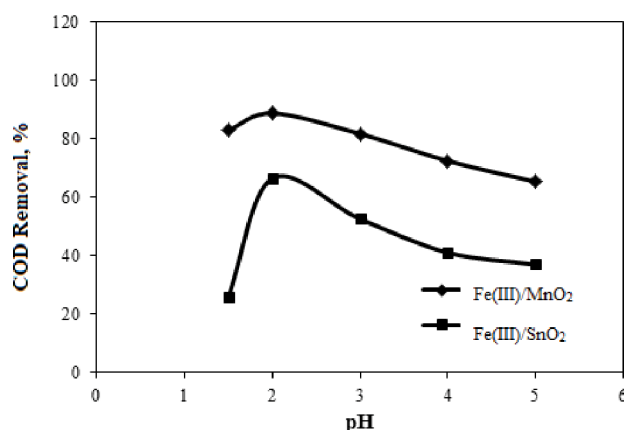


Fig. 6. Effect of the pH on COD removal efficiency (Fe(III)/MnO<sub>2</sub> = 1.5 g/L – Fe(III)/SnO<sub>2</sub> = 2.0 g/L, H<sub>2</sub>O<sub>2</sub> = 200 ppm, temperature 30°C, reaction time 2 h).

directly with H<sub>2</sub>O<sub>2</sub> and consequently reduce the concentration of hydrogen peroxide in the environment [91].



Fe(III)/MnO<sub>2</sub> catalyst and Fe(III)/SnO<sub>2</sub> catalyst gave the highest results with 97.63% color, 88.70% COD and 83.33% color, 66.37% COD removal efficiency at pH 2, respectively. Based on this, the optimum pH value was set at 2. A similar result has been reported by Daud and Hameed [92] as the optimum pH value is 2.

### 3.4. Effect of the hydrogen peroxide concentration on the heterogeneous Fenton process

When examining the effect of hydrogen peroxide concentration on color and COD removal, the hydrogen peroxide concentration was changed from 100 to 400 ppm and the other experimental conditions were kept constant. The result of the experiment is given in Figs. 7 and 8.

When the experiment results obtained with Fe(III)/MnO<sub>2</sub> and Fe(III)/SnO<sub>2</sub> catalysts were examined, it was concluded that both catalysts show a similar tendency with hydrogen peroxide increase. Color and COD removal were increased by up to the most appropriate value (200 ppm) with increasing hydrogen peroxide concentration and then remained stable. The Fe(III)/MnO<sub>2</sub> catalyst gave better results with 97.77% color and 89.01% COD removal.

By increasing the concentration of hydrogen peroxide, more hydrogen peroxide molecules can reach the catalyst surface and react more with iron ions. Thus, the production of hydroxyl radicals increases and the color and COD removal efficiency of the wastewater increase accordingly. When the concentration of hydrogen peroxide is low, a sufficient number of hydroxyl radicals are not produced, resulting in a low oxidation rate [93,94]. But working with high concentrations of hydrogen peroxide, hydrogen peroxide reacts with hydroxyl radicals, causing the hydroxyl radicals in the environment to decrease. The resulting hydroperoxyl radicals also react with the hydroxyl radical to form H<sub>2</sub>O and O<sub>2</sub> [95]. For this reason, it is very important to determine

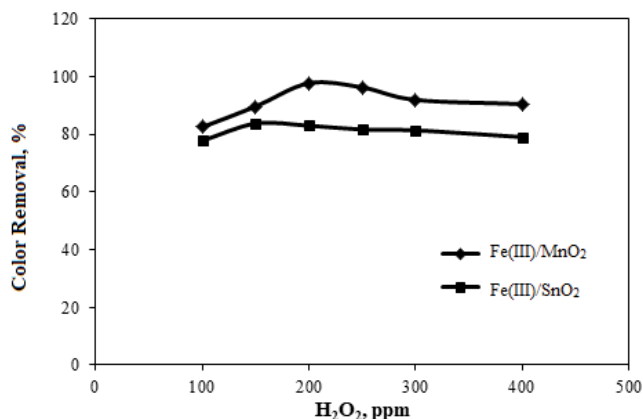


Fig. 7. Effect of the hydrogen peroxide concentration on color removal efficiency (Fe(III)/MnO<sub>2</sub> = 1.5 g/L – Fe(III)/SnO<sub>2</sub> = 2.0 g/L, pH = 2, temperature 30°C, reaction time 2 h).

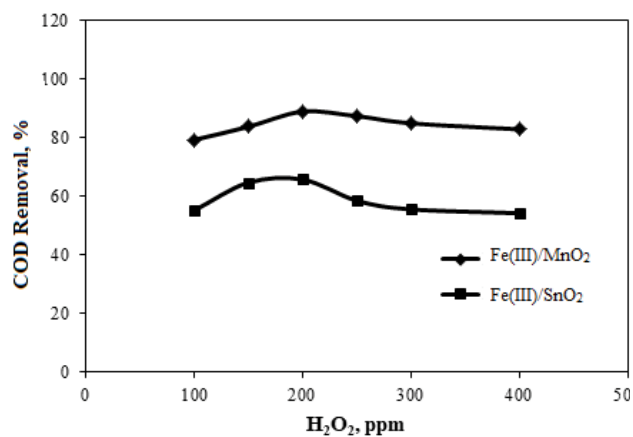


Fig. 8. Effect of the hydrogen peroxide concentration on COD removal efficiency (Fe(III)/MnO<sub>2</sub> = 1.5 g/L – Fe(III)/SnO<sub>2</sub> = 2.0 g/L, pH = 2, temperature 30°C, reaction time 2 h).

the optimum amount of hydrogen peroxide in experimental studies.



ElShafei et al. [96] determined the optimum H<sub>2</sub>O<sub>2</sub> concentration of 333 ppm in their heterogeneous Fenton study. Wu et al. [97] and Liu et al. [98] studied at 250 and 323 ppm H<sub>2</sub>O<sub>2</sub> concentrations as the optimum, respectively.

### 3.5. Effect of the temperature on the heterogeneous Fenton process

To study the effect of the temperature change, the values ranging from 20 to 50°C were studied and the obtained results are given in Figs. 9 and 10. According to the results obtained, when the temperature value increased from 20°C to 30°C, the removal efficiency was also increased. As the temperature increase increases the reaction rate between

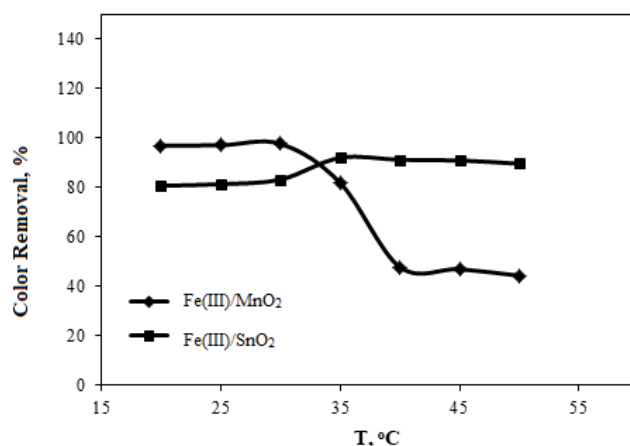


Fig. 9. Effect of temperature on color removal efficiency (Fe(III)/MnO<sub>2</sub> = 1.5 g/L – Fe(III)/SnO<sub>2</sub> = 2.0 g/L, pH = 2, H<sub>2</sub>O<sub>2</sub> = 200 ppm, reaction time 2 h).

the catalyst and hydrogen peroxide, the production rate of hydroxyl radicals also increases [99]. This is confirmed by the law of Arrhenius (reflected on the production rate constant of radicals or by the effect of the same molecules in the degradation of organic molecules) [100].

However, high temperatures generally cause thermal decomposition of hydrogen peroxide to O<sub>2</sub> and H<sub>2</sub>O. This prevents the formation of hydroxyl radicals and reduces the oxidation of organic pollutants [101]. The data obtained from experiments with Fe(III)/MnO<sub>2</sub> catalyst indicates that the color and COD removal efficiency decreased with increasing temperature above 30°C. When the temperature was 30°C, a maximum 97.70% color and 88.87% COD recovery were achieved. The optimum temperature for the Fe(III)/SnO<sub>2</sub> catalyst was determined as 35°C, where 92.07% color and 67.39% COD removal efficiency were obtained.

### 3.6. Effect of the reaction time on the heterogeneous Fenton process

The time of the reaction varied between 5 and 120 min while the previous parameters determined in experimental runs were kept constant and the effect on color and COD removal was investigated.

Reaction kinetics in the process of heterogeneous Fenton are limited to the mass transfer of H<sub>2</sub>O<sub>2</sub> to catalytic activity sites of the catalyst surface. For this reason, heterogeneous Fenton processes have slower reaction kinetics. The longer reaction time of heterogeneous Fenton processes than other AOPs can be explained [12].

The increased reaction time according to Figs. 11 and 12 increased color and COD removal. After 60 min of obtaining the data for the Fe(III)/MnO<sub>2</sub> catalyst, the color, and COD removal remained stable and reached a yield of 88.73% COD and 97.60% color. The optimum reaction time was 120 min for the Fe(III)/SnO<sub>2</sub> catalyst. As for other studies, the reaction time was reported by Yang et al. [102] as 60 min and as 70 min by Wang et al. [27] in their heterogeneous Fenton process using a catalyst. Kakavandi et al. [103] reported 120 min as the optimum reaction time for their study carried



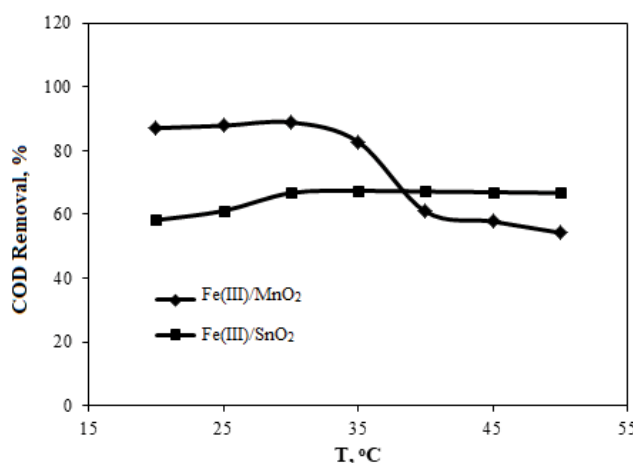


Fig. 10. Effect of temperature on COD removal efficiency (Fe(III)/MnO<sub>2</sub> = 1.5 g/L – Fe(III)/SnO<sub>2</sub> = 2.0 g/L, pH = 2, H<sub>2</sub>O<sub>2</sub> = 200 ppm, reaction time 2 h).

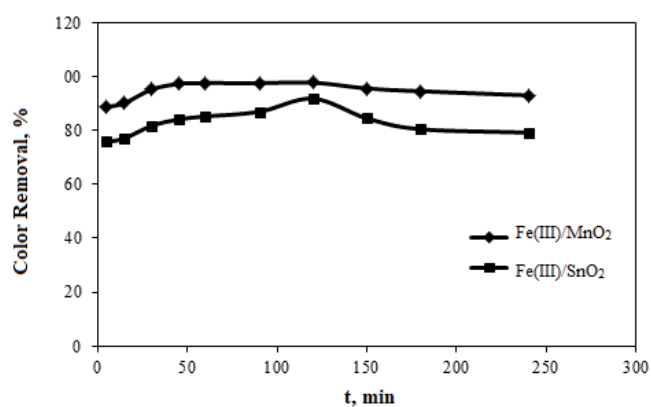


Fig. 11. Effect of reaction time on color removal efficiency (Fe(III)/MnO<sub>2</sub> = 1.5 g/L – Fe(III)/SnO<sub>2</sub> = 2.0 g/L, pH = 2, H<sub>2</sub>O<sub>2</sub> = 200 ppm, temperature for the Fe(III)/MnO<sub>2</sub> catalyst 30°C – temperature for the Fe(III)/SnO<sub>2</sub> catalyst 35°C).

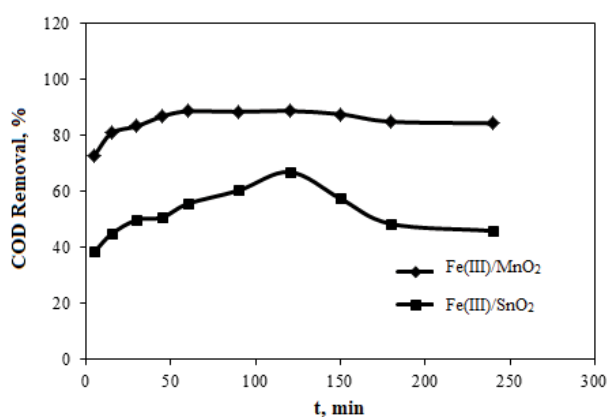


Fig. 12. Effect of reaction time on COD removal efficiency (Fe(III)/MnO<sub>2</sub> = 1.5 g/L – Fe(III)/SnO<sub>2</sub> = 2.0 g/L, pH = 2, H<sub>2</sub>O<sub>2</sub> = 200 ppm, temperature for the Fe(III)/MnO<sub>2</sub> catalyst 30°C – temperature for the Fe(III)/SnO<sub>2</sub> catalyst 35°C).

out with activated carbon/magnetite catalyst. Lopez-Lopez et al. [104]’s reaction time of 120 min reached the removal efficiency.

### 3.7. Effect of the mixing speed on the heterogeneous Fenton process

The effect of the mixing speed on the heterogeneous Fenton process was determined by keeping the experimental parameters fixed and the results are given in Figs. 13 and 14. According to the results obtained from the experiments for mixing speed effect, the color and COD removal efficiency obtained for both catalysts were increased with increasing mixing speed. When operating at 40 rpm mixing

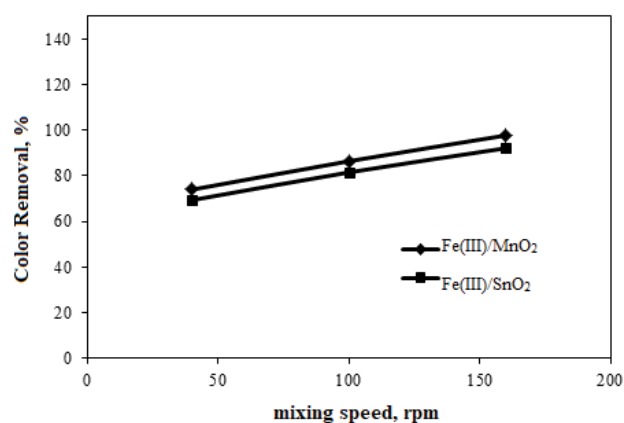


Fig. 13. Effect of mixing speed on color removal efficiency (Fe(III)/MnO<sub>2</sub> = 1.5 g/L – Fe(III)/SnO<sub>2</sub> = 2.0 g/L, pH = 2, H<sub>2</sub>O<sub>2</sub> = 200 ppm, temperature for the Fe(III)/MnO<sub>2</sub> catalyst 30°C – temperature for the Fe(III)/SnO<sub>2</sub> catalyst 35°C, reaction time the Fe(III)/MnO<sub>2</sub> catalyst 60 min – reaction time for the Fe(III)/SnO<sub>2</sub> catalyst 120 min).

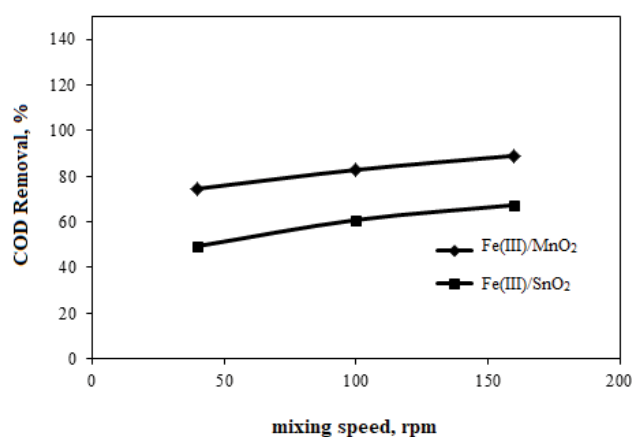


Fig. 14. Effect of mixing speed on COD removal efficiency (Fe(III)/MnO<sub>2</sub> = 1.5 g/L – Fe(III)/SnO<sub>2</sub> = 2.0 g/L, pH = 2, H<sub>2</sub>O<sub>2</sub> = 200 ppm, temperature for the Fe(III)/MnO<sub>2</sub> catalyst 30°C – temperature for the Fe(III)/SnO<sub>2</sub> catalyst 35°C, reaction time the Fe(III)/MnO<sub>2</sub> catalyst 60 min – reaction time for the Fe(III)/SnO<sub>2</sub> catalyst 120 min).



speed, 74.03% color and 74.61% COD removal for Fe(III)/MnO<sub>2</sub> catalyst and 68.43% color and 49.47% COD removal for Fe(III)/SnO<sub>2</sub> catalyst were obtained. When the mixing speed was increased to 160 rpm, 97.80% color and 89.05% COD removal for Fe(III)/MnO<sub>2</sub> catalyst and 92.20% color and 67.43% COD removal efficiency for Fe(III)/SnO<sub>2</sub> catalyst were attained. This can be explained by the homogeneous mixing of the solution and the effective contact of the catalyst and wastewater at the higher mixing speed [99]. The optimum mixing speed was determined as 160 rpm.

### 3.8. Reuse of catalysts

As the reuse of catalyst at wastewater treatment studies is important in terms of cost efficiency, it should be examined in experimental studies. The re-usability of the synthesized Fe(III)/MnO<sub>2</sub> and Fe(III)/SnO<sub>2</sub> catalysts were investigated. Experimental studies were carried out under optimum conditions. Four consecutive experiments were performed for both catalysts. After each experiment, the catalysts were removed from the solution and washed with deionized water several times. They were dried in the oven at 105°C for 24 h. The results of the experiment are given in Table 6. In the fourth experiment, 94.25% color and 85.12% COD removal efficiency for Fe(III)/MnO<sub>2</sub> catalyst and 89.12% color and 64.17% COD removal efficiency for Fe(III)/SnO<sub>2</sub> catalyst were obtained. The results indicate that the activity of the catalyst has gradually decreased during four consecutive runs. The reduction in efficiency is thought to be due to the reduction of this initial activity due to the small amount of iron leaking from the catalyst surface [18].

## 4. Conclusions

In this study, a heterogeneous Fenton process was applied to sunflower oil industry wastewater to investigate color and COD removal efficiency. The parameters affecting the color and COD removal efficiency were examined and the most suitable experimental conditions were secured. Experimental work has been carried out with Fe(III)/MnO<sub>2</sub> and Fe(III)/SnO<sub>2</sub> catalysts containing 8 wt.% Fe(III) ion and the efficiency of these catalysts was compared. The pore sizes of the catalysts we prepared were very close to each other. However, it has been determined that the surface area of the Fe(III)/MnO<sub>2</sub> catalyst is about three times larger than the surface area of the Fe(III)/SnO<sub>2</sub> catalyst. With the Fe(III)/MnO<sub>2</sub> catalyst, 98% color and 89% COD removal was achieved during the reaction lasting for 60 min (optimum

conditions; catalyst amount 1.5 g/L, pH 2, H<sub>2</sub>O<sub>2</sub> = 200 ppm, T = 30°C, 160 rpm). When the Fe(III)/SnO<sub>2</sub> catalyst was used, the reaction time increased to 2 times. At the end of the reaction time of 120 min, 92% color and 67% COD removal efficiency were obtained (optimum conditions; catalyst amount 2.0 g/L, pH 2, H<sub>2</sub>O<sub>2</sub> = 200 ppm, T = 35°C, 160 rpm). The large surface area of the Fe(III)/MnO<sub>2</sub> catalyst compared to Fe(III)/SnO<sub>2</sub> catalyst, increased the number of active areas, thus enabling us to achieve higher color and COD removal efficiency.

Catalysts provide higher iron ion concentration, higher surface area, and more active sites that break down hydrogen peroxide. The most important advantages were that the heterogeneous Fenton processes did not generate waste sludge, that the catalysts could be used repeatedly and they could be easily removed from the environment. The reusability of both catalysts was examined and the results of the experiment showed that color and COD removal efficiency were very high. The use of the iron ion in the heterogeneous phase allows the iron to be readily separated from the solution and allows the catalyst to be reused without significantly losing its effectiveness. In this way, the total cost of the process can be greatly reduced. According to the obtained high yield, the heterogeneous Fenton process was determined as a suitable method for the treatment of wastewater of the sunflower oil industry. The initial investment and operating costs of AOPs are higher than other treatment methods. However, in AOPs, less space is needed compared to other treatment methods; this will allow for more efficient use of the spaces within the plant and thus the operating cost of the treatment plant site will be lower. In further studies, the advantages of AOPs in terms of cost can be examined in detail.

## Acknowledgments

This study was funded by the Scientific Research Projects Commission of Eskişehir Osmangazi University with project number 201615059.

## References

- [1] S.R. Pouran, A.R.A. Aziz, W.M.A.W. Daud, Review on the main advances in photo-Fenton oxidation system for recalcitrant wastewaters, *J. Ind. Eng. Chem.*, 21 (2015) 53–69.
- [2] B. Bethi, S.H. Sonawane, B.A. Bhanvase, S.P. Gumfekar, Nanomaterials-based advanced oxidation processes for wastewater treatment: a review, *Chem. Eng. Process. Process Intensif.*, 109 (2016) 178–189.
- [3] A. Babuponnusami, K. Muthukumar, A review on Fenton and improvements to the Fenton process for wastewater treatment, *J. Environ. Chem. Eng.*, 2 (2014) 557–572.
- [4] A.D. Bokare, W.Y. Choi, Review of iron-free Fenton-like systems for activating H<sub>2</sub>O<sub>2</sub> in advanced oxidation processes, *J. Hazard. Mater.*, 275 (2014) 121–135.
- [5] D.J. Lapworth, N. Baran, M.E. Stuart, R.S. Ward, Emerging organic contaminants in groundwater: a review of sources, fate and occurrence, *Environ. Pollut.*, 163 (2012) 287–303.
- [6] N. Ratola, A. Cincinelli, A. Alves, A. Katsoyiannis, Occurrence of organic microcontaminants in the wastewater treatment process. A mini review, *J. Hazard. Mater.*, 239–240 (2012) 1–18.
- [7] V.L. Tyagi, S.-L. Lo, Application of physico-chemical pre-treatment methods to enhance the sludge disintegration and subsequent anaerobic digestion: an up to date review, *Rev. Environ. Sci. Biotechnol.*, 10 (2011) 215–242.

Table 6  
Reuse of catalysts results

Experiment	Color removal, %		COD removal, %	
	MnO <sub>2</sub>	SnO <sub>2</sub>	MnO <sub>2</sub>	SnO <sub>2</sub>
1	97.80	92.20	89.05	67.43
2	96.42	91.55	88.15	66.23
3	95.23	90.62	86.76	65.20
4	94.25	89.12	85.12	64.11

- [8] P.R. Gogate, A.B. Pandit, A review of imperative technologies for wastewater treatment I: oxidation technologies at ambient conditions, *Adv. Environ. Res.*, 8 (2004) 501–551.
- [9] C. Comninellis, A. Kapalka, S. Malato, S.A. Parsons, I. Poullos, D. Mantzavinos, Advanced oxidation processes for water treatment: advances and trends for R&D, *J. Chem. Technol. Biotechnol.*, 83 (2008) 769–776.
- [10] S. Esplugas, D.M. Bila, L.G.T. Krause, M. Dezotti, Ozonation and advanced oxidation technologies to remove endocrine disrupting chemicals (EDCs) and pharmaceuticals and personal care products (PPCPs) in water effluents, *J. Hazard. Mater.*, 149 (2007) 631–642.
- [11] A.M. Vandenberghe, R. Morent, N. De Geyter, C. Leys, Non-thermal plasmas for non-catalytic and catalytic VOC abatement, *J. Hazard. Mater.*, 195 (2011) 30–54.
- [12] S. Garcia-Segura, L.M. Bellotindos, Y.-H. Huang, E. Brillas, M.-C. Lu, Fluidized-bed Fenton process as alternative wastewater treatment technology—a review, *J. Taiwan Inst. Chem. Eng.*, 67 (2016) 211–225.
- [13] M. Kurian, D.S. Nair, Heterogeneous Fenton behavior of nano nickel zinc ferrite catalysts in the degradation of 4-chlorophenol from water under neutral conditions, *J. Water Process Eng.*, 8 (2015) 37–49.
- [14] A. Cihanoglu, G. Gunduz, M. Dukkanci, Degradation of acetic acid by heterogeneous Fenton-like oxidation over iron-containing ZSM-5 zeolites, *Appl. Catal., B*, 165 (2015) 687–699.
- [15] N.A. Youssef, S.A. Shaban, F.A. Ibrahim, A.S. Mahmoud, Degradation of methyl orange using Fenton catalytic reaction, *Egypt. J. Pet.*, 25 (2016) 317.
- [16] P.H. Sreeja, K.J. Sosamony, A comparative study of homogeneous and heterogeneous photo-Fenton process for textile wastewater treatment, *Procedia Technol.*, 24 (2016) 217.
- [17] W.P. Kwan, B.M. Voelker, Rates of hydroxyl radical generation and organic compound oxidation in mineral-catalyzed Fenton-like systems, *Environ. Sci. Technol.*, 37 (2003) 1150–1158.
- [18] H. Hassan, B.H. Hameed, Fe-clay as effective heterogeneous Fenton catalyst for the decolorization of Reactive Blue 4, *Chem. Eng. J.*, 171 (2011) 912–918.
- [19] A. Khataee, P. Gholami, B. Vahid, Catalytic performance of hematite nanostructures prepared by N<sub>2</sub> glow discharge plasma in heterogeneous Fenton-like process for acid red 17 degradation, *J. Ind. Eng. Chem.*, 50 (2017) 86–95.
- [20] Y.P. Zhang, K.T. Dong, Z. Liu, H.L. Wang, S.X. Ma, A. Zhang, M. Li, L.Q. Yu, Y. Li, Sulfurized hematite for photo-Fenton catalysis, *Prog. Nat. Sci. Mater. Int.*, 27 (2017) 443–451.
- [21] L. Labiadh, M.A. Oturan, M. Panizza, N.B. Hamadi, S. Ammar, Complete removal of AHPs synthetic dye from water using new electro-fenton oxidation catalyzed by natural pyrite as heterogeneous catalyst, *J. Hazard. Mater.*, 297 (2015) 34–41.
- [22] C. Kantar, O. Oral, O. Urken, N.A. Oz, S. Keskin, Oxidative degradation of chlorophenolic compounds with pyrite-Fenton process, *Environ. Pollut.*, 247 (2019) 349–361.
- [23] L.Y. Zeng, J.Y. Gong, J.F. Dan, S. Li, J.D. Zhang, W.H. Pu, C.Z. Yang, Novel visible light enhanced Pyrite-Fenton system toward ultrarapid oxidation of *p*-nitrophenol: catalytic activity, characterization and mechanism, *Chemosphere*, 228 (2019) 232–240.
- [24] C. Kantar, O. Oral, O. Urken, N.A. Oz, Role of complexing agents on oxidative degradation of chlorophenolic compounds by pyrite-Fenton process: batch and column experiments, *J. Hazard. Mater.*, 373 (2019) 160–167.
- [25] O. Oral, C. Kantar, Diclofenac removal by pyrite-Fenton process: performance in batch and fixed-bed continuous flow systems, *Sci. Total Environ.*, 664 (2019) 817–823.
- [26] A.L. Larralde, D. Onna, K.M. Fuentes, E.E. Sileo, M. Hojamberdiev, S.A. Bilmes, Heterogeneous photo-Fenton process mediated by Sn-substituted goethites with altered OH-surface density, *J. Photochem. Photobiol., A*, 381 (2019) 111856.
- [27] Y. Wang, Y.W. Gao, L. Chen, H. Zhang, Goethite as an efficient heterogeneous Fenton catalyst for the degradation of methyl orange, *Catal. Today*, 252 (2015) 107–112.
- [28] Z.-R. Lin, X.-H. Ma, L. Zhao, Y.-H. Dong, Kinetics and products of PCB28 degradation through a goethite-catalyzed Fenton-like reaction, *Chemosphere*, 101 (2014) 15–20.
- [29] T.T.N. Phan, A.N. Nikoloski, P.A. Bahri, D. Li, Enhanced removal of organic using LaF<sub>3</sub>-integrated modified natural zeolites via heterogeneous visible light photo-Fenton degradation, *J. Environ. Manage.*, 233 (2019) 471–480.
- [30] T.X.H. Le, M. Drobek, M. Bechelany, J. Motuzas, A. Julbe, M. Cretin, Application of Fe-MFI zeolite catalyst in heterogeneous electro-Fenton process for water pollutants abatement, *Microporous Mesoporous Mater.*, 278 (2019) 64–69.
- [31] D.S. Bhatkhande, V.G. Pangarkar, A. ACM Beenackers, Photocatalytic degradation for environmental applications - a review, *J. Chem. Technol. Biotechnol.*, 77 (2001) 102.
- [32] M.C. Vagi, A.S. Petsas, Recent advances on the removal of priority organochlorine and organophosphorus biorecalcitrant pesticides defined by Directive 2013/39/EU from environmental matrices by using advanced oxidation processes: an overview (2007–2018), *J. Environ. Chem. Eng.*, (2019), <https://doi.org/10.1016/j.jece.2019.102940>, (In Press).
- [33] A. Fujishima, T.N. Rao, D.A. Tryk, Titanium dioxide photocatalysis, *J. Photochem. Photobiol., C*, 1 (2000) 1–21.
- [34] A. Temirel, S. Palamutcu, Functional textiles III: self-cleaning with photocatalytic effect on textile surfaces, *E-J. Text. Technol.*, 5 (2011) 35–50.
- [35] M.A. Gondal, A. Hameed, Z.H. Yamani, A. Arfaj, Photocatalytic transformation of methane into methanol under UV laser irradiation over WO<sub>3</sub>, TiO<sub>2</sub> and NiO catalysts, *Chem. Phys. Lett.*, 392 (2004) 372–377.
- [36] G.R. Bamwenda, H. Arakawa, The visible light induced photocatalytic activity of tungsten trioxide powders, *Appl. Catal., A*, 210 (2001) 181–191.
- [37] J.M. Poyatos, M.M. Muñoz, M.C. Almecija, J.C. Torres, E. Hontoria, F. Osorio, Advanced oxidation processes for wastewater treatment: state of the art, *Water Air Soil Pollut.*, 205 (2010) 187–204.
- [38] S. Malato, P. Fernández-Ibáñez, M.I. Maldonado, J. Blanco, W. Gernjak, Decontamination and disinfection of water by solar photocatalysis: recent overview and trends, *Catal. Today*, 147 (2009) 1–59.
- [39] A. Darjan, C. Draghici, D. Perniu, A. Duta, Degradation of Pesticides by TiO<sub>2</sub> Photocatalysis, Environmental Security Assessment and Management of Obsolete Pesticides in Southeast Europe, Part of the Series NATO Science for Peace and Security Series C: Environmental Security, Chapter 14, 2013, pp. 155–163.
- [40] S. Ahmed, M.G. Rasul, R. Brown, M.A. Hashib, Influence of parameters on the heterogeneous photocatalytic degradation of pesticides and phenolic contaminants in wastewater: a short review, *J. Environ. Manage.*, 92 (2011) 311–330.
- [41] J. Fenoll, P. Hellín, C.M. Martínez, P. Flores, S. Navarro, Semiconductor-sensitized photodegradation of *s*-triazine and chloroacetanilide herbicides in leaching water using TiO<sub>2</sub> and ZnO as catalyst under natural sunlight, *J. Photochem. Photobiol., A*, 238 (2012) 81–87.
- [42] M.M. Ba-Abbad, M.S. Takriff, M. Said, A. Benamor, M.S. Nasser, A.W. Mohammad, Photocatalytic degradation of pentachlorophenol using ZnO nanoparticles: study of intermediates and toxicity, *Int. J. Environ. Res.*, 11 (2017) 461–473.
- [43] Y.-H. Wang, Z. Zhou, Q.-Y. Chen, J.-L. Zhao, Electrochemical Treatment of Pentachlorophenol on Ni-Sb-SnO<sub>2</sub>/Ti Electrodes, International Symposium on Water Resource and Environmental Protection, 2 (2011) 1379–1381.
- [44] J.F. Niu, Y.P. Bao, Y. Li, Z. Chai, Electrochemical mineralization of pentachlorophenol (PCP) by Ti/SnO<sub>2</sub>-Sb electrodes, *Chemosphere*, 92 (2013) 1571–1577.
- [45] V.G.G. Kanmoni, S. Daniel, G.A.G. Raj, Photocatalytic degradation of chlorpyrifos in aqueous suspensions using nanocrystals of ZnO and TiO<sub>2</sub>, *React. Kinet. Catal. Lett.*, 106 (2012) 325–339.
- [46] G.C. Pathiraja, M.S. Wijesingha, N. Nanayakkara, Ti/IrO<sub>2</sub>/SnO<sub>2</sub> anode for electrochemical degradation of chlorpyrifos in water:

- optimization and degradation Performances, IOP Conf. Ser.: Mater. Sci. Eng., 201 (2017) 012040.
- [47] A. Eslami, M. Hashemi, F. Ghanbari, Degradation of 4-chlorophenol using catalyzed peroxymonosulfate with nano-MnO<sub>2</sub>/UV irradiation: toxicity assessment and evaluation for industrial wastewater treatment, *J. Cleaner Prod.*, 195 (2018) 1389–1397.
- [48] Y. He, D.B. Jiang, D.Y. Jiang, J. Chen, Y.X. Zhang, Evaluation of MnO<sub>2</sub>-templated iron oxide-coated diatomites for their catalytic performance in heterogeneous photo Fenton-like system, *J. Hazard. Mater.*, 344 (2018) 230–240.
- [49] W.X. Zhang, Z.H. Yang, X. Wang, Y.C. Zhang, X.G. Wen, S.H. Yang, Large-scale synthesis of β-MnO<sub>2</sub> nanorods and their rapid and efficient catalytic oxidation of methylene blue dye, *Catal. Commun.*, 7 (2006) 408–412.
- [50] N. Sui, Y.Z. Duan, X.L. Jiao, D.R. Chen, Large-scale preparation and catalytic properties of one-dimensional α/β-MnO<sub>2</sub> nanostructures, *J. Phys. Chem. C*, 113 (2009) 8560–8565.
- [51] J. Howsawkung, A.L. Teel, T.F. Hess, R.L. Crawford, R.J. Watts, Simultaneous abiotic reduction–biotic oxidation in a microbial-MnO<sub>2</sub>-catalyzed Fenton-like system, *Sci. Total Environ.*, 409 (2010) 439–445.
- [52] A.L.-T. Pham, F.M. Doyle, D.L. Sedlak, Inhibitory effect of dissolved silica on H<sub>2</sub>O<sub>2</sub> decomposition by iron(III) and manganese(IV) oxides: implications for H<sub>2</sub>O<sub>2</sub>-based in situ chemical oxidation, *Environ. Sci. Technol.*, 46 (2012) 1055–1062.
- [53] G.S. Cao, L. Su, X.J. Zhang, H. Li, Hydrothermal synthesis and catalytic properties of α- and β-MnO<sub>2</sub> nanorods, *Mater. Res. Bull.*, 45 (2010) 425–428.
- [54] N.A. Fathy, S.E. El-Shafey, O.I. El-Shafey, W.S. Mohamed, Oxidative degradation of RB19 dye by a novel γ-MnO<sub>2</sub>/MWCNT nanocomposite catalyst with H<sub>2</sub>O<sub>2</sub>, *J. Environ. Chem. Eng.*, 1 (2013) 858–864.
- [55] O. Furman, D.F. Laine, A. Blumenfeld, A.L. Teel, K. Shimizu, I.F. Cheng, R.J. Watts, Enhanced reactivity of superoxide in water-solid matrices, *Environ. Sci. Technol.*, 43 (2009) 1528–1533.
- [56] F.R. Spellman, *Water and Wastewater Treatment Plant Operations*, CRS Press, Taylor & Francis Group, Boca Raton, Florida, 2014, 851 p.
- [57] A. Tan, *Some Pollution in Wastewater Examination of Parameters*, Master's Thesis, Trakya University, Turkey, 2006.
- [58] I. Ozturk, H. Timur, U. Koşkan, *Domestic, Industrial Wastewater Treatment and Control of Sewage Sludge*, Principles of Wastewater Treatment, Turkey, 2005.
- [59] H.F. David, B.G. Liptak, P.A. Bouis, *Groundwater and Surface Water Pollution*, CRC Press, Lewis Publisher, Boca Raton, Florida, 2000.
- [60] F.I. Hai, K. Yamamoto, K. Fukushi, Hybrid treatment systems for dye wastewater, *Crit. Rev. Env. Sci. Technol.*, 37 (2007) 315–377.
- [61] S. Aslan, B. Alyüz, Z. Bozkurt, M. Bakaoğlu, Characterization and biological treatability of edible oil wastewaters, *Pol. J. Environ. Stud.*, 18 (2009) 533–538.
- [62] K. Vijayaraghavan, D. Ahmad, M.E.B.A. Aziz, Aerobic treatment of palm oil mill effluent, *J. Environ. Manage.*, 82 (2007) 24–31.
- [63] Y. Saatci, E.I. Arslan, V. Konar, Removal of total lipids and fatty acids from sunflower oil factory effluent by UASB reactor, *Bioresour. Technol.*, 87 (2003) 269–272.
- [64] N. Azbar, T. Yonar, Comparative evaluation of a laboratory and full-scale treatment alternatives for the vegetable oil refining industry wastewater (VORW), *Process Biochem.*, 39 (2004) 869–875.
- [65] Y.O. Fouad, Separation of cottonseed oil from oil–water emulsions using electrocoagulation technique, *Alexandria Eng. J.*, 53 (2014) 199–204.
- [66] U.T. Un, A.S. Kopalal, U.B. Ogutveren, Electrocoagulation of vegetable oil refinery wastewater using aluminum electrodes, *J. Environ. Manage.*, 90 (2009) 428–433.
- [67] M. Cheryan, N. Rajaopalan, Membrane processing of oily streams. Wastewater treatment and waste reduction, *J. Membr. Sci.*, 151 (1998) 13–28.
- [68] F.L. Hua, Y.F. Tsang, Y.J. Wang, S.Y. Chan, H. Chua, S.N. Sin, Performance study of ceramic microfiltration membrane for oily wastewater treatment, *Chem. Eng. J.*, 128 (2007) 169–175.
- [69] T. Mohammadi, A. Esmaelifar, Wastewater treatment using ultrafiltration at a vegetable oil factory, *Desalination*, 166 (2004) 329–337.
- [70] T. Mohammadi, A. Esmaelifar, Wastewater treatment of a vegetable oil factory by a hybrid ultrafiltration-activated carbon process, *J. Membr. Sci.*, 254 (2005) 129–137.
- [71] M. Decloux, M.-L. Lameloise, A. Brocard, E. Bisson, M. Parmentier, A. Spiraers, Treatment of acidic wastewater arising from the refining of vegetable oil by crossflow microfiltration at very low transmembrane pressure, *Process Biochem.*, 42 (2007) 693–699.
- [72] H. Moazed, T. Viraraghavan, Removal of oil from water by bentonite organoclay. *Pract. Period. Hazard. Toxic Radioact. Waste Manage.*, 9 (2005) 130–134.
- [73] M.G. Devi, Z.S.S. Al-Hashmi, G.C. Sekhar, Treatment of vegetable oil mill effluent using crab shell chitosan as adsorbent, *Int. J. Environ. Sci. Technol.*, 9 (2012) 713–718.
- [74] D. Mysore, T. Viraraghavan, Y.-C. Jin, Treatment of oily waters using vermiculite, *Water Res.*, 39 (2005) 2643–2653.
- [75] Y. Asci, M. Cam, Treatment of synthetic dye wastewater by using Fe/CuO particles prepared by co-precipitation: parametric and kinetic studies, *Desal. Wat. Treat.*, 73 (2017) 281–288.
- [76] N.-Y. He, J.-M. Cao, S.-L. Bao, Q.-H. Xu, Room-temperature synthesis of an Fe-containing mesoporous molecular sieve, *Mater. Lett.*, 31 (1997) 133–136.
- [77] A. Taguchi, F. Schüth, Ordered mesoporous materials in catalysis, *Microporous Mesoporous Mater.*, 77 (2005) 1–45.
- [78] E.F. Yüksel, Examination of Microporous Solids, M.Sc. Thesis Ankara University, Turkey, 2005, 73 p.
- [79] A. Khataee, S. Fathinia, M. Fathinia, Production of pyrite nanoparticles using high energy planetary ball milling for sonocatalytic degradation of sulfasalazine, *Ultrason. Sonochem.*, 34 (2017) 904–915.
- [80] J.J. Zhang, X.H. Zhang, Y.F. Wang, Degradation of phenol by a heterogeneous photo-Fenton process using Fe/Cu/Al catalysts, *RSC Adv.*, 6 (2016) 13168–13176.
- [81] A. Khataee, P. Gholami, M. Sheydaei, Heterogeneous Fenton process by natural pyrite for removal of a textile dye from water: effect of parameters and intermediate identification, *J. Taiwan Inst. Chem. Eng.*, 58 (2016) 366–373.
- [82] L.J. Xu, J.L. Wang, Magnetic Nanoscaled Fe<sub>3</sub>O<sub>4</sub>/CeO<sub>2</sub> Composite as an efficient fenton-like heterogeneous catalyst for degradation of 4-chlorophenol, *Environ. Sci. Technol.*, 46 (2012) 10145–10153.
- [83] B.X. Zhao, X. Li, W. Li, L. Yang, J.C. Li, W.X. Xia, L. Zhou, F. Wang, C. Zhao, Degradation of trichloroacetic acid by an efficient Fenton/UV/TiO<sub>2</sub> hybrid process and investigation of synergetic effect, *Chem. Eng. J.*, 273 (2015) 527–533.
- [84] B. Muthukumari, K. Selvam, I. Muthuvel, M. Swaminathan, Photoassisted hetero-Fenton mineralisation of azo dyes by Fe(II)-Al<sub>2</sub>O<sub>3</sub> catalyst, *Chem. Eng. J.*, 153 (2009) 9–15.
- [85] J. Herney-Ramirez, M.A. Vicente, L.M. Madeira, Heterogeneous photo-Fenton oxidation with pillared clay-based catalysts for wastewater treatment: a review, *Appl. Catal., B*, 98 (2010) 10–26.
- [86] F. Ji, C.L. Li, J.H. Zhang, L. Deng, Efficient decolorization of dye pollutants with LiFe(WO<sub>4</sub>)<sub>2</sub> as a reusable heterogeneous Fenton-like catalyst, *Desalination*, 269 (2011) 284–290.
- [87] S. Karthikeyan, A. Titus, A. Gnanamani, A.B. Mandal, G. Sekaran, Treatment of textile wastewater by homogeneous and heterogeneous Fenton oxidation processes, *Desalination*, 281 (2011) 438–445.
- [88] F. Martínez, G. Calleja, J.A. Melero, R. Molina, Heterogeneous photo-Fenton degradation of phenolic aqueous solutions over iron-containing SBA-15 catalyst, *Appl. Catal., B*, 60 (2005) 181–190.
- [89] M.A. Zazouli, F. Ghanbari, M. Yousefi, S. Madihi-Bidgoli, Photocatalytic degradation of food dye by Fe<sub>3</sub>O<sub>4</sub>-TiO<sub>2</sub> nanoparticles in presence of peroxymonosulfate: the effect of UV sources, *J. Environ. Chem. Eng.*, 5 (2017) 2459–2468.
- [90] M. Ahmadi, F. Ghanbari, Combination of UVC-LEDs and ultrasound for peroxymonosulfate activation to degrade synthetic dye: influence of promotional and inhibitory agents

- and application for real wastewater, *Environ. Sci. Pollut. Res.*, 25 (2018) 6003–6014.
- [91] N. Jaafarzadeh, F. Ghanbari, M. Moradi, Photo-electro-oxidation assisted peroxymonosulfate for decolorization of acid brown 14 from aqueous solution, *Korean J. Chem. Eng.*, 32 (2015) 458–464.
- [92] N.K. Daud, B.H. Hameed, Fenton-like oxidation of reactive black 5 solution using iron–Montmorillonite K10 catalyst, *J. Hazard. Mater.*, 176 (2010) 1118–1121.
- [93] A.A. Babaei, B. Kakavandi, M. Rafiee, F. Kalantarhormizi, I. Purkaram, E. Ahmadi, S. Esmaeili, Comparative treatment of textile wastewater by adsorption, Fenton, UV-Fenton and US-Fenton using magnetic nanoparticles-functionalized carbon (MNP@C), *J. Ind. Eng. Chem.*, 56 (2017) 163–174.
- [94] L.S. Luo, Y.Y. Yao, F. Gong, Z.F. Huang, W.Y. Lu, W.X. Chen, L. Zhang, Drastic enhancement on Fenton oxidation of organic contaminants by accelerating Fe(III)/Fe(II) cycle with L-cysteine, *RSC Adv.*, 6 (2016) 47661–47668.
- [95] L.J. Xu, J.L. Wang, Fenton-like degradation of 2,4-dichlorophenol using Fe<sub>3</sub>O<sub>4</sub> magnetic nanoparticles, *Appl. Catal., B*, 123–124 (2012) 117–126.
- [96] G.M.S. ElShafei, F.Z. Yehia, O.I.H. Dimitry, A.M. Badawi, Gh. Eshaq, Extending the working pH of nitrobenzene degradation using ultrasonic/heterogeneous Fenton to the alkaline range via amino acid modification, *Chemosphere*, 139 (2015) 632–637.
- [97] Y. Wu, S.L. Zeng, F.F. Wang, M. Megharaj, R. Naidu, Z.L. Chen, Heterogeneous Fenton-like oxidation of malachite green by iron-based nanoparticles synthesized by tea extract as a catalyst, *Sep. Purif. Technol.*, 154 (2015) 161–167.
- [98] Y. Liu, D. Sun, Effect of CeO<sub>2</sub> doping on catalytic activity of Fe<sub>2</sub>O<sub>3</sub>/γ-Al<sub>2</sub>O<sub>3</sub> catalyst for catalytic wet peroxide oxidation of azo dyes, *J. Hazard. Mater.*, 143 (2006) 448–454.
- [99] C.P. Bai, W.Q. Gong, D.X. Feng, M. Xian, Q. Zhou, S.H. Chen, Z.X. Ge, Y.H. Zhou, Natural graphite tailings as heterogeneous Fenton catalyst for the decolorization of rhodamine B, *Chem. Eng. J.*, 197 (2012) 306–313.
- [100] L.F. Guerreiro, C.S.D. Rodrigues, R.M. Duda, R.A. de Oliveira, R.A.R. Boaventura, L.M. Madeira, Treatment of sugarcane vinasse by combination of coagulation/flocculation and Fenton's oxidation, *J. Environ. Manage.*, 181 (2016) 237–248.
- [101] M. Karatas, Y.A. Argun, M.E. Argun, Decolorization of antraquinonic dye, Reactive Blue 114 from synthetic wastewater by Fenton process: kinetics and thermodynamics, *J. Ind. Eng. Chem.*, 18 (2012) 1058–1062.
- [102] B. Yang, Z. Tian, L. Zhang, Y.P. Guo, S.Q. Yan, Enhanced heterogeneous Fenton degradation of Methylene Blue by nanoscale zero valent iron (nZVI) assembled on magnetic Fe<sub>3</sub>O<sub>4</sub>/reduced graphene oxide, *J. Water Process Eng.*, 5 (2015) 101–111.
- [103] B. Kakavandi, A. Takdastan, N. Jaafarzadeh, M. Azizi, A. Mirzaei, A. Azari, Application of Fe<sub>3</sub>O<sub>4</sub>@C catalyzing heterogeneous UV-Fenton system for tetracycline removal with a focus on optimization by a response surface method, *J. Photochem. Photobiol., A*, 314 (2016) 178–188.
- [104] C. Lopez-Lopez, J. Martín-Pascual, M.V. Martínez-Toledo, M.M. Muñoz, E. Hontoria, J.M. Poyatos, Kinetic modelling of TOC removal by H<sub>2</sub>O<sub>2</sub>/UV, photo-Fenton and heterogeneous photocatalysis processes to treat dye-containing wastewater, *Int. J. Environ. Sci. Technol.*, 12 (2015) 3255–3262.